Metrological traceability of a digital 3-axis MEMS accelerometers sensor network

Towards the metrological traceability of a sensor network and the trustworthiness of data provided: a case study on 25 digital MEMS accelerometers

Andrea Prato[1], *Fabrizio Mazzoleni*[1], *Giulio D'Emilia*[2], *Antonella Gaspari*[2], *Emanuela Natale*[2], *Alessandro Schiavi*[1]

[1] *INRiM - Istituto Nazionale di Ricerca Metrologica, 10135 Torino, Italy*

[2] *University of L'Aquila, Department of Industrial and Information Engineering and of Economics, 67100 L'Aquila, Italy*

Corresponding author e-mail: *a.prato@inrim.it*

Abbreviated title: Metrological traceability of a sensor network

Abstract

Digital MEMS sensor networks are nowadays widely applied in environmental and manufacturing applications. However, fundamental metrological requirements, such as traceability and trustworthiness of data, are often disregarded by manufacturers and end-users. In this work, traceability of a sensor network prototype, composed of 25 digital 3-axis MEMS accelerometers, conceived for structural monitoring at low-frequencies, is investigated. Main and transverse sensitivities are provided for each axis at three low-frequencies by two laboratories with recently-developed independent vibration calibration systems using inclined planes. Comparison of the 225 main sensitivities shows compatible results. Given the large amount of data to be managed by end-users, the possibility of decreasing its number is then investigated by managing sensitivity and uncertainty data according to different combinations of three examined factors, i.e. MEMS, frequency and axis. Thus, the number of data is reduced at the expense of higher uncertainties but preserving the traceability and the trustworthiness of sensors data.

Keywords: Vibration calibration, Digital Sensors, Network sensitivity, MEMS, Trustworthiness, Traceability.

1. Introduction

Nowadays systems for survey, monitoring and control based on digital MEMS sensor networks has become a widely established practice in many application and engineering fields. The ease of use, flexibility, low-cost and low-power consuming of MEMS sensors, together with the enhanced big data flows managing and the digitalization, have made these "technological sensing infrastructures" very attracting tools to detect a great variety of physical quantities, processes and phenomena, from the small-scale up to the large-scale (until the Earth-scale). Besides, the development of new technologies based on independent devices and communications, such as IoT in each different implementation, from healthcare to smart industries, from domotics to autonomous driving, is based on the deployment of very complex wide distributed grids of sensors.

However, by referring to the terminology defined in VIM [1] and in [2], some typical metrological attributes of measuring instruments, such as traceability, accuracy and the trustworthiness of data provided, are often disregarded for MEMS sensors, applied in the nodes of networks. «Trustworthiness of measurements» represents in a comprehensive and very communicative way the measurement quality level, under several technical points of view [3, 4].

Sometimes, end-users implement custom calibration techniques (or more properly, custom adjustments) or rely on the calibration data provided by the manufacturers, without traceable methods. Depending on the applications (more or less sensitive), it may be necessary to actually have traceable and accurate data, or at least data-sets expressed within well-defined confidence levels. It follows that a traceable network of sensors is certainly more trustworthy (and much more competitive) than ordinary networks, since data supplied can be considered effectively representative of measured phenomena, beyond to be compatible and reproducible.

In order to amend this lack, some applicative protocols begin to be published, e.g., by IEEE Standard Association [5] providing common framework for sensor performance specification terminology, units, conditions, and limits. Indeed, the large deployment of sensors with digital output and network systems needs to be underpinned by new metrological approaches (such as remote self-calibration, data aggregation in network systems and uncertainty analysis) allowing to support trustworthy and safe operation, linked to traceability chains, to guarantee higher quality management requirements.

The relevance of these emerging needs in the field of metrology, has recently oriented the strategy plan of BIPM [6], in order to «identify and deliver the highest impact opportunities to support National Metrology Institutes (NMIs) priorities in, for example, the areas of "big data" and digital transformation», as well as several consultative committees within it [7-10], with the aim to provide suitable calibration procedures for these systems, against national primary standards, and to provide the traceability chain to the national laboratories and to the manufacturers, at present not yet available.

In Fig. 1 the metrological traceability chain and the path of the International System of Units propagation, through subsequent calibrations, from primary standard to end-users, is schematically represented.

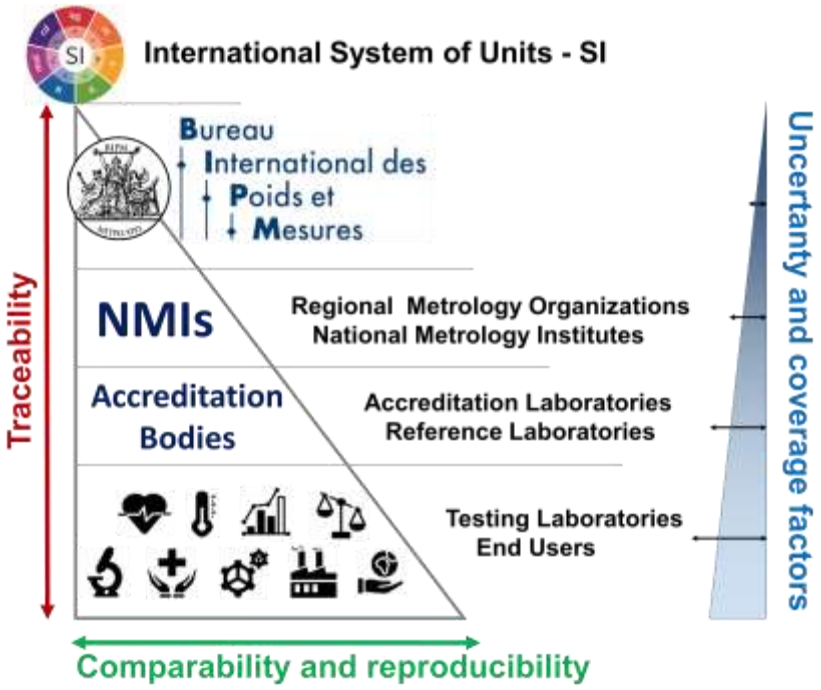

Fig. 1. The metrological traceability chain and the propagation of the SI.

As a consequence, there are not still technical standards for the calibration of sensors with digital output and digital interface, thus end-users will usually get neither a calibration certificate nor a traceability statement from the manufacturer, although the sensitivity is adjusted during the production process. As it is known, in some applications there are several legal or insurance reasons for which it is preferable to use sensors calibrated in accredited and certified laboratories, according to the ISO 17025 standard [11].

In the frame of the Strategy 2019 to 2029 of the Consultative Committee for Acoustics, Ultrasound, and Vibration at BIPM, the vision is strongly oriented to the issue of digitalization and to the traceability of sensors with digital interfaces, since markets are generating the basic components to enable to development of low-cost robust sensor systems capable of wireless, autonomous and intelligent operation, possibly combining multi-parameter sensing within a single device or network of devices. Indeed, the metrology applied to sensor networks, under several points of view, is particularly stimulated from both industrial needs and sensors manufacturers, and several NMIs worldwide are planning their activities along these perspectives. From a general survey beyond specific applications, in USA at NIST, security, trust and trustworthiness of sensors applied in networks and in distributed system for Internet of Things (IoT) and Network of Things (NoT), are investigated [12]; in Germany at PTB, the role of metrology for the digitalization of the economy and society in the digital age is studied [13]; in Italy at INRIM, within an integrated industrial partnership network [14], the processes of knowledge transfer, supporting the traceability chain to sensors with digital outputs, are applied for environment, industry and smart manufacturing [15-20].

Within the framework of the European Association of National Metrology Institutes (EURAMET), this topic is widely debated and several proposals are developed within joint research projects, such as “Metrology

for the Factory of the Future" (Met4FoF) [21], "Metrology for the next-generation digital substation instrumentation" (FutureGrid II) [22] or "Communication and validation of smart data in IoT-networks" (SmartCom) [23], among others.

The metrological research devoted to the sensor networks, intended as the whole infrastructure – i.e., from the acquisition systems (sensing elements, nodes), to the systems for transferring, processing and distributing signals (microcontrollers), to the transmission and connectivity protocols, to the collecting hubs, up to the end-user – is a wide field of investigation, aimed to provide trustworthy and traceable data, within suitable coverage factors and uncertainties budgets, tailored to the actual needs of specific applications and employments, and a multidisciplinary effort of different competences has to be harmonized, steps by steps. In Fig. 2 the description of a simplified sensor network infrastructure and the related metrological needs are depicted.

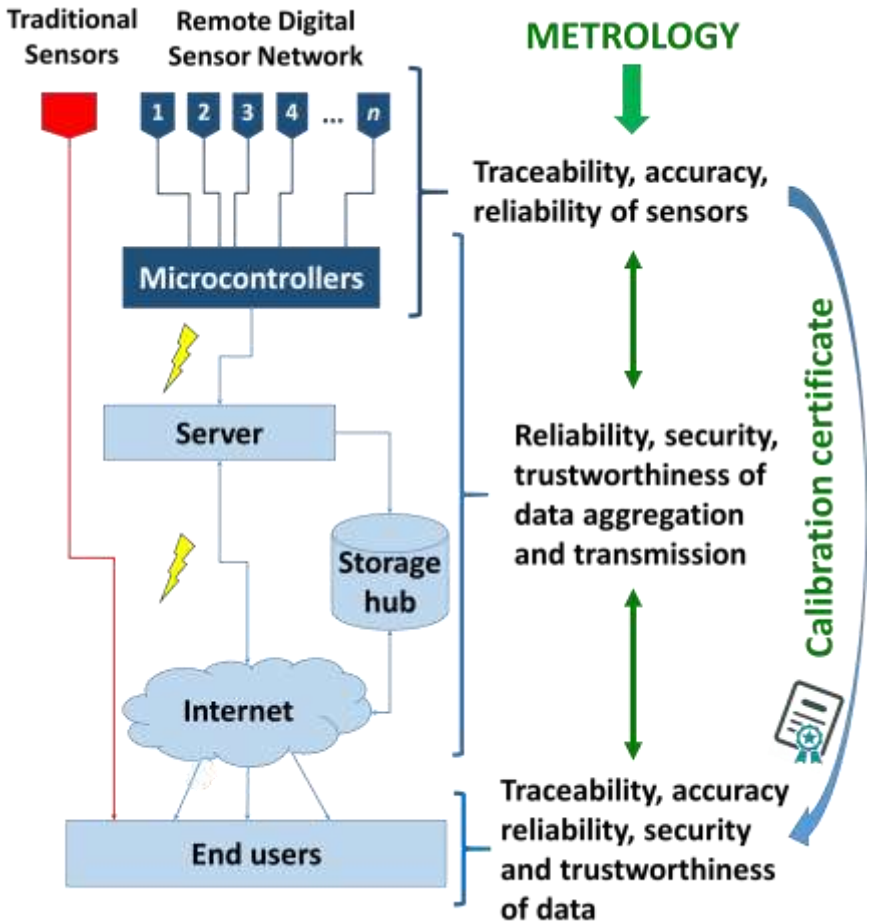

Fig. 2. The sensor network infrastructure and the metrological needs.

The first fundamental step, from a metrological perspective towards the traceability of a sensor network as a whole, is founded on the trustworthiness of data provided by the single sensors employed, once properly calibrated, thus on the ability to provide measurement uncertainty and/or quality information together with the

measurement data. Nevertheless, since «these technologies have different mounting requirements, use different testing and calibration protocols, and use digital interfaces for data and communications» [7], it is not always possible to completely fulfill the current standard requirements for the calibration; on the other hand, some different analyses and limitations need to be applied, in order to identify and quantify the actual sensitivity values of digital sensors. In addition, standard calibration methods are not feasible in terms of timings and costs, compatibly with the low-cost of the sensors.

In the case of digital MEMS accelerometers, the sensitivity is generally provided by the manufacturer without traceable methods and sometimes it is estimated in static conditions. Dynamic response, as a function of frequency, is often unknown. On the other hand, traceable calibration methods for digital sensors, including sensitivity parameter and uncertainty analysis are necessary, in order to consider digital MEMS accelerometers as actual measurement devices in the frequency domain [24-27]. For these reasons, two independent calibration systems using tilted plates suitable for MEMS accelerometers have been developed by INRIM (National Institute of Metrological Research) [28-29] and UNIVAQ (University of L'Aquila) [30-33].

2. Material and methods

In this work, as a case-study, the traceability and the reproducibility of sensors to be employed in a network, composed of 25 digital 3-axis MEMS accelerometers, nominally identical, are investigated. Each sensor is calibrated by comparison to INRIM secondary standard (previously calibrated against INRIM primary standard), to establish the first link to the metrological traceability chain. In this way, the traceability is assured, and the robustness of compatibility and reproducibility is verified on the basis of a bilateral comparison between INRIM and UNIVAQ. It is worth noting that in relevant standards, calibration of rectilinear vibration transducers is mainly intended for the evaluation of magnitude sensitivity and optionally for phase shift sensitivity. Therefore, in the following, calibration measurements are related to the first case. Traceability of the sensors, to be applied within the network, is provided through calibration methods by comparison to a calibrated reference transducer: the actual main sensitivity, in frequency domain, of each axis for each single MEMS accelerometer, and the transverse sensitivities, due to the mutual interactions among axes, are accurately quantified. Experimental results, obtained from the two independent dynamic calibration systems and procedures in terms of "digitized sensitivities", are then verified and finally compared to each other and with the nominal sensitivity provided by the manufacturer [34]. The analyzed MEMS accelerometers are a part of the same production batch, provided by manufacturer (STMicroelectronics). Calibration results of the 25 MEMS accelerometers are then compared and experimental expanded uncertainties are used to evaluate the sensitivity ranges of the MEMS accelerometers, with suitable coverage factors, in order to estimate the trustworthiness of data provided by the sensors within the network, employed by end-users. The sensors under investigation are the sensing elements of a network-prototype, conceived for structural and infrastructures health monitoring and for seismic safety networks at urban/building scale, suitable for low-frequency range vibration measurements [35-39].

2.1 Sensitivity and sensors

2.1.1 «Digitized» Sensitivity

First of all, it is necessary to define a proper sensitivity parameter for digital outputs. According to the IEEE Standard for digital accelerometer [5], the sensitivity is defined in terms of Least Significant Bit (LSB) referred to g, i.e., g/LSB. The change in acceleration input corresponding to 1 LSB change in output. This definition is widely used in digital sensors datasheets. Nevertheless, in our opinion, the use of term LSB is partially confusing for digital outputs for two main reasons. First, the actual digital output value is a n bit 0/1 binary sequence, converted into a decimal number (Decimaln-bit). Second, although 1 LSB corresponds to 20=1 Decimal$_{n\text{-}bit}$ in most of the cases, according to IEEE Standard, it is not always true, since 1 LSB could correspond to other bit positions, i.e. 21=2 Decimal$_{n\text{-}bit}$, 22=4 Decimal$_{n\text{-}bit}$, or more. Therefore, in the following, the «digitized sensitivity» of a digital MEMS accelerometer is expressed, in linear units, as Decimal$_{n\text{-}bit}$/(m s^{-2}) (or simply D$_{n\text{-}bit}$/(m s^{-2})), by analogy to typical sensitivity of analog accelerometers, expressed in linear units, in terms of V/(m s^{-2}). The n-bit subscript indicates the number of bits to which the Decimal refers to, i.e. 12-bit, 16-bit, depending on the standard used by the device.

2.1.2 Sensor network sensitivity

The definition of sensor network sensitivity could be misleading when compared to the traditional concept of sensitivity. In fact, traditionally, the sensitivity, together with the associated uncertainty, is provided to each individual sensor by varying the main parameters of influence (e.g., frequencies and axes, in the case of accelerometers), with the result that several quantities are related to a single transducer. However, in the case of sensor networks, that may consist of tens, hundreds, if not thousands of transducers, attributing sensitivity to each transducer and for each parameter of influence might be difficult to manage in numerical, computational and consuming terms by end-users in actual applications [40–43], particularly at present time in which manufacturers usually do not provide traceable sensitivities [27]. By way of example, in the case of triaxial accelerometer transducers, the sensitivity is usually provided for each single axis of sensitivity for different frequencies, at a specific oscillation amplitude. Therefore, as a lower estimate, from 9 (3 frequencies × 3 main axes) to 36 (12 frequencies × 3 main axes) sensitivity values are attributed to each sensor (neglecting the possible variability with amplitude and the evaluation of the transverse sensitivities). Projecting this count to a small network of 25 sensors, as in this case, an amount of sensitivity data ranging from 225 to 900 is obtained. Despite the small size of this MEMS accelerometers network, however, such number of data might be difficult to manage by the end-user, with the risk of compromising the trustworthiness of data provided by the network if the end-user, in order to reduce the number of sensitivities to manage, has no experience in handling these data with a metrological approach, in terms of mean sensitivity values and propagation of the associated uncertainties. Therefore, before drafting a traceability protocol, it is important to consider this aspect in order to evaluate what kind of and how many sensitivity data should be provided to the end-users, commensurate with the size and final application of the sensor network, that ensure its optimal trustworthiness.

In this case study, therefore, beside evaluating the sensitivity of all 25 MEMS in terms of main (and transverse) sensitivities for each single axis and for each tested frequency (225 main sensitivity values in total), the possibility to provide a lower number of sensitivity values with associated uncertainties, from the case of axis- and frequency-independent sensitivity for each MEMS (25 sensitivity values) to the limit case of a single sensitivity value independent from MEMS, axis and frequency, is investigated, as it will be shown in Section IV.

2.1.3 The digital 3-axis MEMS accelerometer

The 25 digital 3-axis MEMS accelerometers investigated in this work (Fig. 3) are commercial low-power digital MEMS accelerometers (ST, model LSM6DSR [34]). The device is composed of an accelerometer sensor, a charge amplifier, and an analog-to-digital converter. The digital MEMS accelerometers are connected by a serial cable to a separated external microcontroller, in which other electronic components are integrated. In this comparison the same external microcontroller (ST, model 32F769IDISCOVERY [44]), to acquire the digital samples and to provide the required power supply to the MEMS accelerometer, is used.

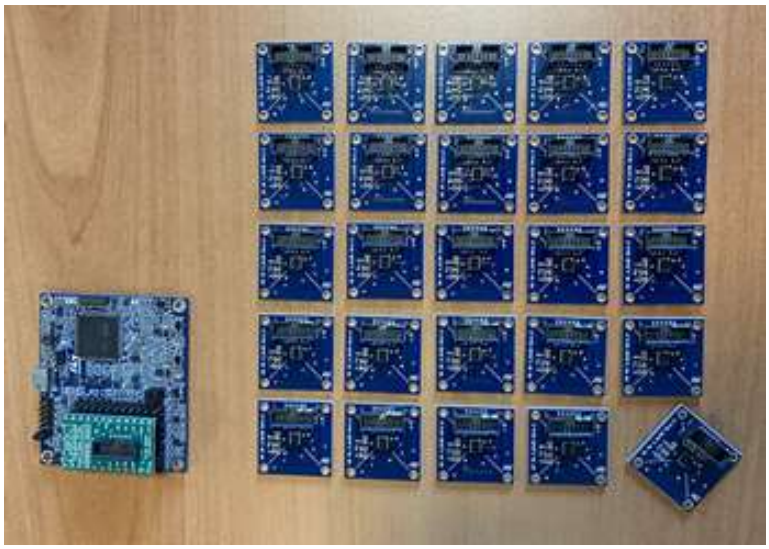

Fig. 3. The set of 25 digital 3-axis MEMS accelerometers and the microcontroller.

The microcontroller has from 3 to 5 Serial Peripheral Interfaces (SPIs) available, and, to each one, it is possible to connect up to 8/10 sensors. Therefore, it is technically possible to connect from 20 to 40 sensors for each microcontroller, without introducing complications (such as other electronic components) [45]. However, in real cases, as for the present case of structural and infrastructures health monitoring at urban/building scale, different microcontrollers should be used. As a matter of fact, the maximum MEMS-microcontroller distance depends on the interface and data speed. With an SPI interface and considering only one sensor, a 2 m cable, suitable for building scales, can be used. By increasing the number of sensors on the same channel, the transfer speed has to be increased, thus the length of the cable has to be reduced. Therefore, at building

scale, it would only be practical for such MEMS sensors to have a dedicated microcontroller and network the microcontrollers. However, since, as a first step, the aim is to provide traceability to single sensors independently of the adopted microcontrollers, calibration is performed by connecting the microcontroller to a single MEMS.

The signal is acquired by means of a SPI, which is a synchronous serial communication interface used for connecting digital sensors together. The 1-bit signal from the ΣΔ-ADC is then converted through a decimation process and a low pass filter into a standard 16-bit-signed PCM (Pulse Code Modulation) signal with a nominal sampling frequency rate of 1660 Hz. According to the manufacturer [45], however, sampling frequencies up to -6% of the target, i.e. up to 1560 Hz, can be expected. For this reason, the actual sampling frequency of every MEMS, as shown in Fig. 4, is previously evaluated by counting the number of points of the known generated sinusoidal signals, in order to perform accurate calibration measurements. Sampling frequencies range from around 1580 Hz to 1630 Hz.

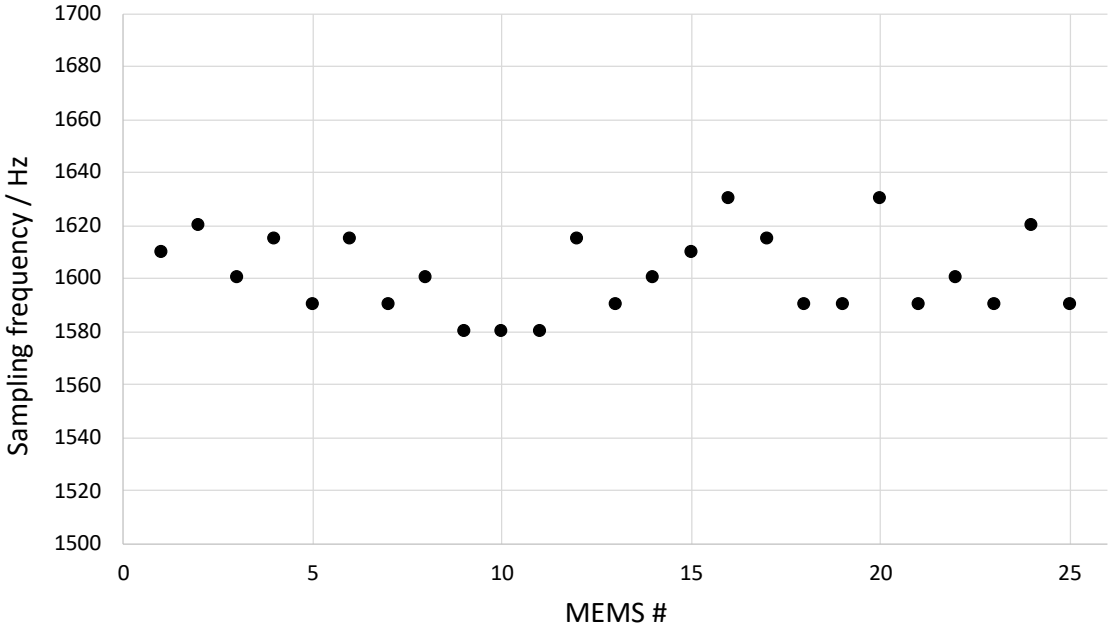

Fig. 4. The actual sampling frequency of the 25 digital 3-axis MEMS accelerometers.

The amplitude values range between -2^{16-1}=-32768 $D_{16\text{-bit-signed}}$ and $+(2^{16-1}-1)$ =+32767 $D_{16\text{-bit-signed}}$, where the digit unit is a signed 16-bit sequence converted into a decimal number.

The linear acceleration sensitivity of a digital MEMS accelerometer, expressed by manufacturer in terms of mg/LSB, depends on the "full scale" used in testing condition, and it is conventionally attributed to every sensitive axis of the sensor, for static and dynamic measurements, independently from frequency, without any indication about the associated uncertainty, and is not evaluated thought traceable calibration methods. In this work, by using a "full scale" of ±2 g, the sensitivity declared is 0.061 mg/LSB.

In decimal units, it corresponds to 0.061 mg/$D_{16\text{-bit-signed}}$, i.e. 0.598×10^{-3} (m s^{-2})/$D_{16\text{-bit-signed}}$. As commonly used in analogue transducers, the sensitivity is expressed as a function of the reference quantity, thus it properly corresponds to 1671 $D_{16\text{-bit-signed}}$ /(m s^{-2}).

2.2 Calibration procedure

The calibration procedure and the related metrological characterization of the set of 25 sensors is aimed at verifying the actual amplitude response in dynamics, as a function of frequency, on the basis of the bilateral comparison between laboratories. The procedure is based on a calibration by comparison, with a reference accelerometer (in analogy to ISO Standard 16063-21 [46]), in order to provide the first "connection" to the primary standard and to verify its transferability, through the secondary standards, to the sensors under investigation. In order to avoid further sources of uncertainty, the calibration of the 25 MEMS is performed by using the same external microcontroller, in both laboratories, although the influence of the microcontrollers in terms of systematic errors and uncertainty contribution, is negligible [45].

Calibration is carried out at in a low frequency range, namely 3 Hz, 6 Hz and 10 Hz, by comparison to a reference transducer. A sinusoidal mechanical dynamic excitation is generated along a single-axis, by means of linear vibrating tables (according to the laboratory equipment), at nearly constant peak amplitude of 1 m s-2. The reference acceleration aref is measured by a reference accelerometer, previously calibrated against INRiM primary standard. In order to simultaneously calibrate the three sensitive axes of the sensors, measurements are performed on inclined planes which allow to generate the projection of the single-axis excitation acceleration, along three sensitive axes (a_x, a_y, a_z) simultaneously, as schematically shown in Fig. 5, according to the laboratory setups and specific procedures.

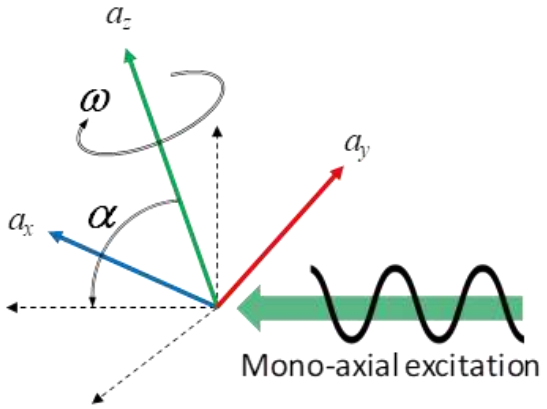

Fig. 5. The schematic principle of the simultaneous 3-axis calibration, with respect to a single-axis of excitation.

In time domain, 100 cycles of oscillation, for each frequency of calibration, are taken into account for the determination of output data. The 3-axis digital MEMS accelerometer under investigation is fixed to the center

of the vibrating table at known angles of rotation ω and at different tilt angles α, with respect to the direction of the single-axis excitation.

The detailed uncertainty budget is evaluated by both laboratories according to GUM [47], taking into account to the sensitivity equations and the related uncertainty contributions peculiar of each calibration system.

2.3 The experimental method and uncertainty assessment

The calibration aims at quantifying, as a function of frequency, the average main sensitivities S_{ii}, as well as the related dispersion of the 25 MEMS accelerometers within opportune coverage factors, and the occurring transversal sensitivities S_{ij}, due to the possible mutual interaction among axes. As a matter of facts, in particular for low-cost sensors, the outputs interact with each other and transverse sensitivities might play a crucial role, unlike in traditional high-quality accelerometers. The three sensitivity axes of the MEMS accelerometer are located with a certain tilt angle α, and a certain rotation angle ω, with respect to the direction of the excitation. The experimental calibration systems are designed and independently realized in each laboratory, as described in detail in [28-33].

2.3.1 INRIM

The calibration setup realised at INRIM consists of a single-axis vibrating table, on which aluminium inclined planes are screwed (Fig. 6). More details can be found in [28].

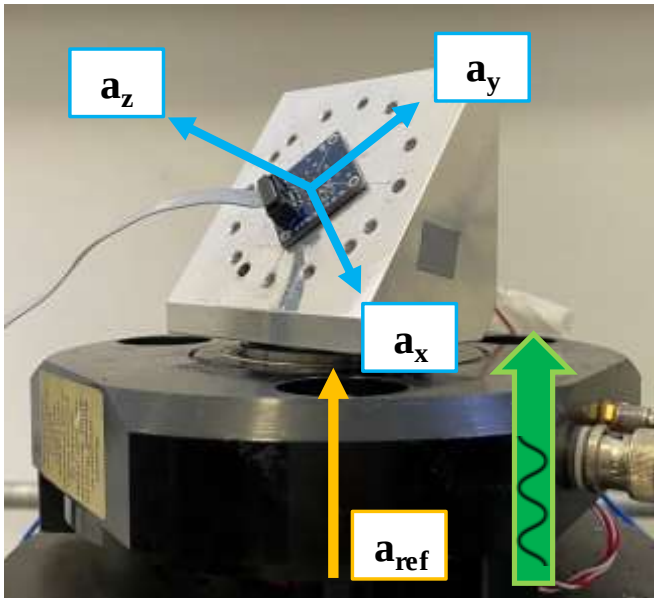

Fig. 6. Calibration setup used at INRIM laboratory.

The digital MEMS accelerometer is fixed to the inclined plane, along the axis of excitation, allowing to generate a projection of the excitation acceleration along the three axes of the MEMS simultaneously. The reference acceleration a_{ref}, corresponding to the sinusoidal excitation acceleration, is measured by a single axis

transducer (PCB model 080A199/482A23, calibrated against INRIM primary standard), integrated in the stroke of the vertical shaker (PCB Precision Air Bearing Calibration Shaker), for the calibration at 6 Hz and 10 Hz. For the calibration at 3 Hz, a single axis horizontal linear slide (APS ELECTRO-SEIS shaker) is used and the reference acceleration is measured by means of laser-Doppler velocimetry (Polytec OFV 505). The reference acceleration is acquired by an acquisition board NI 4431 (sampling rate of 50 kHz) integrated in the PC and processed through LabVIEW® software to provide the Root Mean Square (RMS) reference value in m s^{-2}. In this way, the reference accelerations along the MEMS axes can be found according to:

$$a_x = \left|a_{ref} \sin\alpha \cos\omega\right| \quad (1)$$

$$a_y = \left|a_{ref} \sin\alpha \sin\omega\right| \quad (2)$$

$$a_z = \left|a_{ref} \cos\alpha\right| \quad (3)$$

where, α is the tilt angle, ω is the angle of rotation, a_{ref} is the RMS reference acceleration along the vertical axis *z'* of the excitation system, and a_x, a_y, a_z are the RMS reference accelerations spread along *x*-, *y*- and *z*-axis of the MEMS accelerometer. Measurements are performed in four configurations at different angles of rotation ω and tilt α (α=0° and ω=270°; α=15° and ω=90°; α=75° and ω=0°; α=75° and ω=90°). These configurations are chosen since calibration results are compatible with those obtained from 48 configurations as detailed in [48]. Systematic effects, due to spurious components acting on the perpendicular plane with respect to the excitation axis caused by vibrational modes of the inclined aluminum plates and due to horizontal motions of the shaker, are quantified in terms of amplitude and phase, by means of Laser-Doppler velocimetry (Polytec OFV 505), and corrected for each inclined plane and for all frequencies, as described in detail in [28].

The digital MEMS output is acquired by the external microcontroller and saved as binary files. These files are then processed with MATLAB® software: the digital value for each specific frequency *f* is obtained by applying a first-order Butterworth band-pass filter, centred at the frequency of interest with a fractional band-width of 10%, to the temporal signals and, subsequently, by computing the Root Mean Square (RMS), in order to remove the off-set due to gravity and the influence of background vibrations.

The 3-axis digital MEMS accelerometer outputs d_i (expressed in $D_{16bit\text{-}signed}$), are calculated in matrix form, as a linear combination of the acceleration component in m s^{-2}, as shown in (4), where the main sensitivities S_{ii} and transverse sensitivities S_{ij} are directly obtained from the elements of the sensitivity matrix **S**:

$$[d_x \quad d_y \quad d_z] = [a_x \quad a_y \quad a_z] \cdot \begin{vmatrix} S_{xx} & S_{xy} & S_{xz} \\ S_{yx} & S_{yy} & S_{yz} \\ S_{zx} & S_{zy} & S_{zz} \end{vmatrix} \quad (4)$$

For each MEMS, sensitivity uncertainty matrix **U(S)** (at a confidence level of 95%) is obtained from the covariance matrix of the independent variables by applying the general rule of random error propagation in matrix form [28]. Independent variables, are schematically shown in Fig.7.

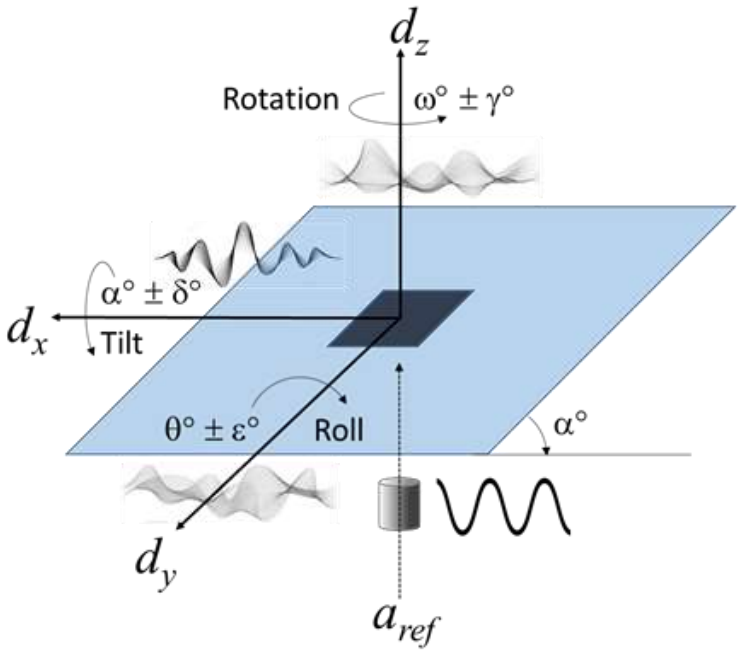

Fig. 7. Schematic representation of uncertainties in INRIM calibration setup.

Independent variables are represented by the reference acceleration a_{ref}, tilt angle α, rotation angle ω, roll angle θ, and by the systematic terms $a_{x',syst}$, $a_{y',syst}$, $a_{z',syst}$ and $\varphi_{x',syst}$, $\varphi_{y',syst}$, $\varphi_{z',syst}$ which are the amplitudes and the phase differences, with respect to the reference signal a_{ref}, of the spurious components affecting the accuracy of the MEMS output d_x, d_y and d_z. Uncertainty contribution ε due to the roll angle θ, nominally 0°, is considered negligible.

Standard uncertainty $u(a_{ref})$ associated to the reference acceleration along the z'-axis of the excitation system derives from the Calibration and Measurement Capabilities (CMC) declared by INRIM [49], which is 0.8% in terms of relative expanded uncertainty from 5 Hz to 1 kHz. At 3 Hz, it is increased to 1%. Standard uncertainties associated to tilt angle $u(\alpha)$, rotation angle $u(\omega)$, considered as type B uncertainty contributions with half-widths δ=0.1°, γ=1°, respectively, and spurious components, $u(a_{x',syst})$, $u(a_{y',syst})$, $u(a_{z',syst})$, $u(\varphi_{x',syst})$, $u(\varphi_{y',syst})$, $u(\varphi_{z',syst})$, are evaluated according to [28].

By way of example, the detailed uncertainty budget for the a_x reference acceleration at an inclination of 75°, a rotation of 90° and a frequency of 6 Hz, is shown in Table I.

Table 1

Uncertainty table of reference acceleration along x-axis at an inclination of 75°, a rotation of 0° and a frequency of 6 Hz.

Variable x_k				$u^2(x_k)$	c_k	$u_k^2(a_x)$
Symb.	Value	Unit	Note			
a_{ref}	0.707	ms^{-2}	Cmc	8,1E-06	9,7E-01	7,6E-06
α	75	°	Acc.	3,3E-03	3,6E-03	4,3E-08
ω	0	°	Acc.	3,3E-01	3,1E-05	3,1E-10
$a_{x',syst}$	0.011	ms^{-2}	Rep.	1,9E-06	-2,6E-01	1,3E-07
$a_{y',syst}$	0.002	ms^{-2}	Rep.	1,9E-06	0,0E+00	0,0E+00
$a_{z',syst}$	0.048	$m\ s^{-2}$	Rep.	1,9E-06	9,7E-01	1,8E-06
$\varphi_{x',syst}$	173.04	°	Rep.	4,0E+00	-6,2E-06	1,5E-10
$\varphi_{y',syst}$	-0.77	°	Rep.	4,0E+00	0,0E+00	0,0E+00
$\varphi_{z',syst}$	0.01	°	Rep.	4,0E+00	4,1E-07	6,7E-13
a_x	0.727	$m\ s^{-2}$		Variance, $u^2(a_x)$		9,5E-06

2.3.1 UNIVAQ

The calibration set-up realised at University of L'Aquila, consisting of a single-axis horizontal vibrating table on which an aluminium hollow inclined plane with a tilt angle of 45° is screwed, generates a projection of the horizontal slide acceleration along three MEMS axes simultaneously (Fig. 8). More details can be found in [33].

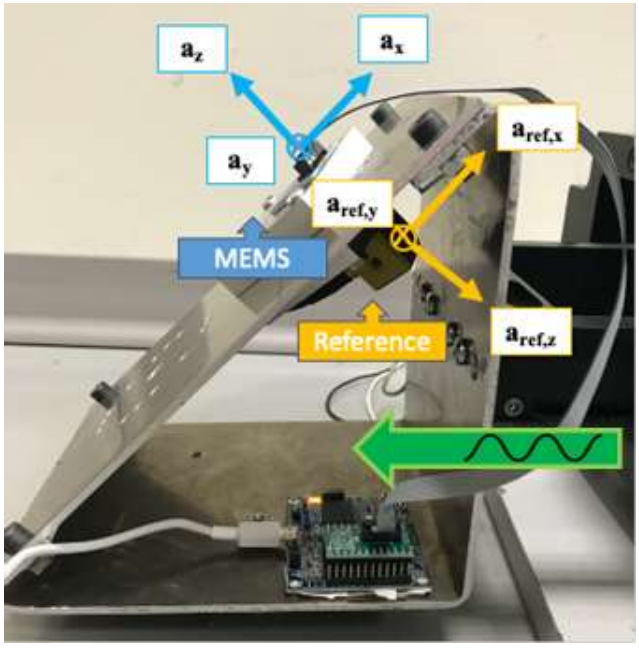

Fig. 8. Calibration setup used at UNIVAQ laboratory

The reference acceleration a_{ref}, provided by a tri-axial piezoelectric accelerometer (PCB model TLD356B18), and the MEMS accelerometer under test are coaxially installed on the two opposite sides of the 45° inclined plane surface, so that their axes are aligned. Measurements are performed in three configurations by placing the MEMS and the reference accelerometer at three angles of rotation ω (0°, 30° and 330°). Single sinusoidal signals are generated by a horizontal linear slide (APS 113 ELECTRO-SEIS shaker). Reference accelerometer signal is acquired by CompactRio 9040 by National Instruments. MEMS output is acquired by the external microcontroller and saved in binary file. Both MEMS and reference acceleration signals are processed by performing an FFT analysis. The amplitudes of the spectrum in the range, centred at the oscillation frequency with a width of ±10%, are added up, in order to prevent eventual variability of sampling frequency of the MEMS. Since the axes of the reference tri-axial accelerometer are nominally coaxial with those of the MEMS accelerometer under investigation (i.e., $a_i = |a_{ref,i}|$), the main sensitivities S_{ii} are obtained by dividing the MEMS digital output d_i values and the measured reference accelerations $a_{ref,i}$, as follows:

$$\begin{cases} S_{xx} = |d_x / a_{ref,x}| \\ S_{yy} = |d_y / a_{ref,y}| \\ S_{zz} = |d_z / a_{ref,z}| \end{cases} \tag{5}$$

By analogy, the values of transverse sensitivities S_{ij} are calculated as $S_{ij} = d_i / |a_{ref,j}|$ by generating sinusoidal accelerations along each sensitivity axis and measuring the MEMS response along the other two orthogonal axes, simultaneously. In Fig. 9 a schematic rapresentation of uncertanty due to the independent variables, is shown.

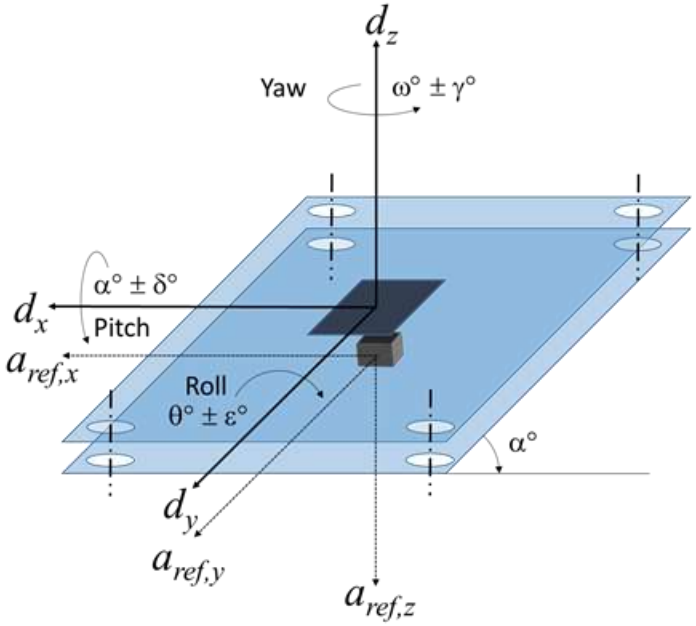

Fig. 8. Schematic representation of uncertainties in UNIVAQ calibration setup

For each MEMS under investigation, the evaluation of the sensitivity expanded uncertainties $U(S_{ij})$ (at a confidence level of 95%) is carried out by considering the reproducibility standard deviations of the three configurations at three different angles of rotation and the uncertainty of the reference accelerometer; the uncertainty of the coaxiality, between MEMS axes and reference accelerometer axes, is estimated with a yaw angle $\gamma°=\pm1°$ on the rotation angle ω and a pitch angle $\delta°=\pm1°$ on the tilt angle α, while the uncertainty due to the roll angle θ, nominally 0°, can be considered negligible. Standard uncertainty $u(a_{ref})$ of the reference accelerations, in terms of relative expanded uncertainty, is 2% at 3 Hz and 6 Hz, and 1.5% at 10 Hz according to the calibration certificate. By way of example, the detailed uncertainty budget of sensitivity along y-axis of MEMS #22 at a rotation angle of 30° and at a frequency of 3 Hz, is shown in Table II

Table 2

Uncertainty table of MEMS #22 sensitivity along Y-axis at a rotation angle of 30 °and at a frequency of 3 Hz.

Variable x_k				$u^2(x_k)$	c_k	$u_k^2(S_y)$
Symb.	Value	Unit	Note			
$a_{ref,y}$	0,50	ms^{-2}	Cert.	2,5E-03	-3,3E+02	2,8E+02
ω	45	°	Acc.	3,3E-01	-5,0E+01	8,4E+02
α	30	°	Acc.	3,3E-01	-2,9E+01	2,8E+02
			Repr.	2,1E+03	1,0E+00	2,1E+03
S_{yy}	1657	$D_{16bit}/(m/s^2)$		Variance, $u^2(S_y)$		3,5E+03

3. Experimental results

Experimental results of the 25 MEMS accelerometers from the two laboratories, at 3 Hz, 6 Hz and 10 Hz, in terms of main sensitivities values along *x*-, *y*- and *z*-axis, and related expanded uncertainties (at a confidence level of 95%), expressed in $D_{16\text{-bit-signed}}/(m/s^2)$, are collected in Tables 3 and 4 (with mean values *m*, standard deviation *s*, and maximum value *M*) and summarized in Figs. 10 and 11.

In general, from a first qualitative point of view, both laboratories show quite uniform main sensitivity values among the 25 MEMS at the different frequencies under investigation, and are close to manufacturer sensitivity of 1671 $D_{16\text{-bit-signed}}/(m/s^2)$, which is nominally referred to all sensitivity axes and for all frequencies without the associated uncertainty. Expanded uncertainties at INRiM are in the order of 2%-4%, while at and UNIVAQ are in the order of 2%-6% with S_{yy} showing higher uncertainty values due to higher reproducibility standard deviations among the configurations. In both laboratories, uncertainties associated to S_{zz} are lower than the opposite axes due to the lower number of independent variables involved. It is also worth noting that

standard deviations between the 25 MEMS sensitivity values (as average, around 13 $D_{16\text{-bit-signed}}/(m\,s^{-2})$) are lower than the calibration standard uncertainties (as average, around 35 $D_{16\text{-bit-signed}}/(m\,s^{-2})$).

Table 3

Main sensitivities with expanded uncertainties (k=2) of the 25 MEMS at INRIM. Values are expressed in $D_{16\text{-bit-signed}}/(m\,s^{-2})$.

#	3 Hz			6 Hz			10 Hz		
	S_{xx}	S_{yy}	S_{zz}	S_{xx}	S_{yy}	S_{zz}	S_{xx}	S_{yy}	S_{zz}
1	1658±56	1667±59	1691±37	1649±57	1657±59	1665±36	1653±57	1649±58	1678±37
2	1666±58	1653±57	1666±36	1650±58	1628±57	1650±36	1643±58	1628±57	1644±36
3	1691±59	1651±59	1687±37	1635±57	1653±59	1650±36	1663±57	1641±58	1660±36
4	1691±59	1693±59	1683±37	1630±57	1639±57	1648±36	1637±57	1642±57	1668±36
5	1672±58	1668±58	1680±37	1665±58	1628±57	1653±36	1664±58	1649±59	1658±36
6	1673±59	1700±61	1675±36	1647±58	1653±59	1643±36	1637±58	1641±59	1654±36
7	1660±58	1666±60	1669±36	1628±57	1647±59	1651±36	1639±57	1654±59	1661±36
8	1645±56	1683±60	1675±36	1625±57	1634±59	1652±36	1650±58	1653±59	1655±36
9	1665±58	1670±59	1693±37	1616±57	1639±58	1680±37	1647±58	1625±59	1666±36
10	1688±59	1667±59	1693±37	1626±57	1653±59	1675±36	1645±57	1644±59	1674±36
11	1685±58	1663±59	1672±36	1661±58	1634±58	1655±36	1639±57	1622±57	1647±36
12	1681±59	1670±59	1679±37	1656±59	1616±58	1669±36	1656±58	1634±59	1663±36
13	1672±58	1659±59	1694±37	1644±58	1630±58	1674±36	1633±57	1633±59	1670±36
14	1692±60	1697±60	1698±37	1670±59	1664±59	1648±36	1675±59	1637±59	1668±36
15	1685±59	1685±60	1682±37	1647±58	1652±59	1667±36	1636±57	1636±59	1655±36
16	1695±60	1680±60	1691±37	1661±59	1644±58	1660±36	1656±58	1635±59	1656±36
17	1686±59	1659±56	1685±37	1659±58	1640±56	1638±36	1642±57	1630±55	1651±36
18	1669±58	1669±59	1687±37	1635±58	1664±59	1677±37	1644±58	1647±59	1672±36
19	1678±58	1676±60	1708±37	1676±58	1657±59	1678±37	1650±57	1655±59	1674±37
20	1672±59	1666±59	1689±37	1666±59	1621±58	1669±36	1654±58	1640±59	1672±36
21	1666±59	1667±59	1695±37	1661±59	1667±59	1640±36	1659±59	1651±59	1656±36
22	1679±60	1673±60	1683±37	1622±58	1626±58	1640±36	1653±58	1649±59	1657±36
23	1680±59	1692±60	1699±37	1654±58	1632±58	1667±36	1658±58	1660±59	1677±37
24	1690±59	1670±59	1680±37	1648±58	1666±59	1635±36	1642±57	1641±59	1657±36
25	1657±57	1680±58	1684±37	1652±58	1641±57	1649±36	1617±56	1633±56	1670±36
m	1676	1673	1686	1647	1643	1657	1648	1641	1663
s	13	13	10	16	15	14	12	10	9
M	60	61	37	59	59	37	59	59	37

Table 4

Main sensitivities with expanded uncertainties (k=2) of the 25 MEMS at UNIVAQ. Values are expressed in $D_{16\text{-bit-signed}}/(m\,s^{-2})$.

#	3 Hz			6 Hz			10 Hz		
	S_{xx}	S_{yy}	S_{zz}	S_{xx}	S_{yy}	S_{zz}	S_{xx}	S_{yy}	S_{zz}
1	1693±65	1701±80	1732±45	1668±65	1681±79	1708±44	1646±62	1660±76	1692±37
2	1692±50	1715±102	1697±44	1675±50	1700±102	1681±43	1680±45	1706±100	1690±37
3	1698±49	1711±74	1703±44	1671±49	1685±72	1680±43	1661±45	1677±69	1671±37
4	1692±50	1721±77	1713±44	1678±48	1705±76	1700±44	1659±43	1683±72	1683±37
5	1711±47	1724±67	1712±45	1679±48	1695±66	1682±43	1672±44	1689±62	1677±37
6	1694±49	1710±89	1705±43	1681±51	1701±90	1692±43	1676±45	1695±88	1691±36
7	1694±60	1724±126	1715±46	1679±58	1709±126	1702±44	1673±54	1702±126	1698±38
8	1698±52	1728±101	1712±44	1670±51	1702±99	1687±43	1654±45	1686±97	1673±37
9	1691±52	1704±101	1709±44	1677±52	1692±102	1697±44	1671±47	1683±100	1694±37
10	1692±51	1708±101	1717±44	1666±51	1681±98	1694±44	1654±45	1667±96	1684±37
11	1692±51	1705±87	1706±44	1664±50	1681±88	1680±43	1655±46	1672±85	1673±37
12	1688±52	1713±76	1698±44	1674±49	1702±76	1688±43	1673±46	1698±73	1690±37
13	1688±50	1719±103	1730±45	1661±50	1693±101	1704±44	1647±47	1679±97	1692±38
14	1690±58	1752±120	1704±44	1679±54	1741±122	1694±44	1668±51	1727±115	1686±37
15	1686±51	1729±112	1705±44	1663±51	1709±110	1685±43	1671±48	1717±108	1695±37
16	1717±51	1692±82	1707±45	1693±51	1670±81	1686±44	1688±47	1668±80	1682±37
17	1708±53	1720±101	1715±44	1681±52	1697±97	1689±43	1671±47	1686±95	1685±37
18	1710±53	1717±101	1717±45	1676±52	1688±97	1686±43	1669±47	1684±94	1682±37
19	1704±51	1728±97	1721±46	1689±50	1714±97	1707±42	1684±45	1710±94	1705±38
20	1705±49	1713±73	1713±44	1688±47	1699±74	1699±44	1672±42	1683±69	1685±37
21	1703±51	1739±98	1710±44	1688±49	1724±99	1697±44	1669±44	1704±98	1680±38
22	1687±49	1726±98	1707±45	1662±50	1704±98	1685±43	1667±44	1708±96	1692±37
23	1717±48	1648±86	1710±45	1694±49	1739±90	1679±43	1688±45	1735±87	1677±37
24	1697±47	1761±94	1691±45	1677±48	1737±94	1671±45	1680±44	1735±97	1676±39
25	1696±55	1712±114	1714±45	1676±54	1694±114	1696±44	1676±48	1693±115	1698±38
m	1698	1717	1711	1676	1702	1691	1669	1694	1686
s	9	21	9	9	18	10	11	20	9
M	65	126	46	65	126	45	62	126	39

435

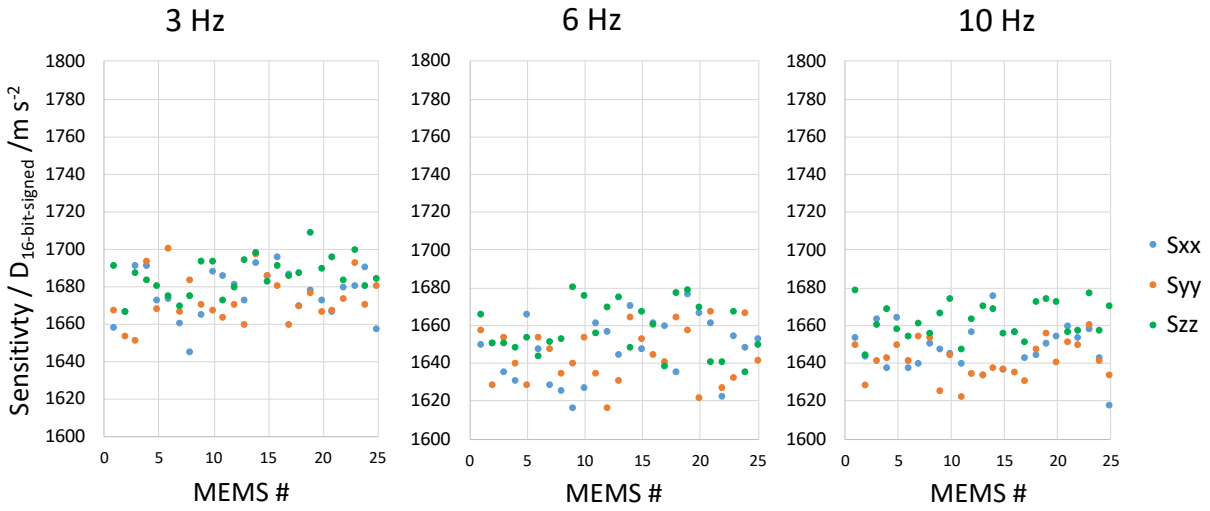

436

437 **Fig. 10**. Main sensitivities of the 25 MEMS at 3 Hz, 6 Hz and 10 Hz evaluated at INRIM.

438

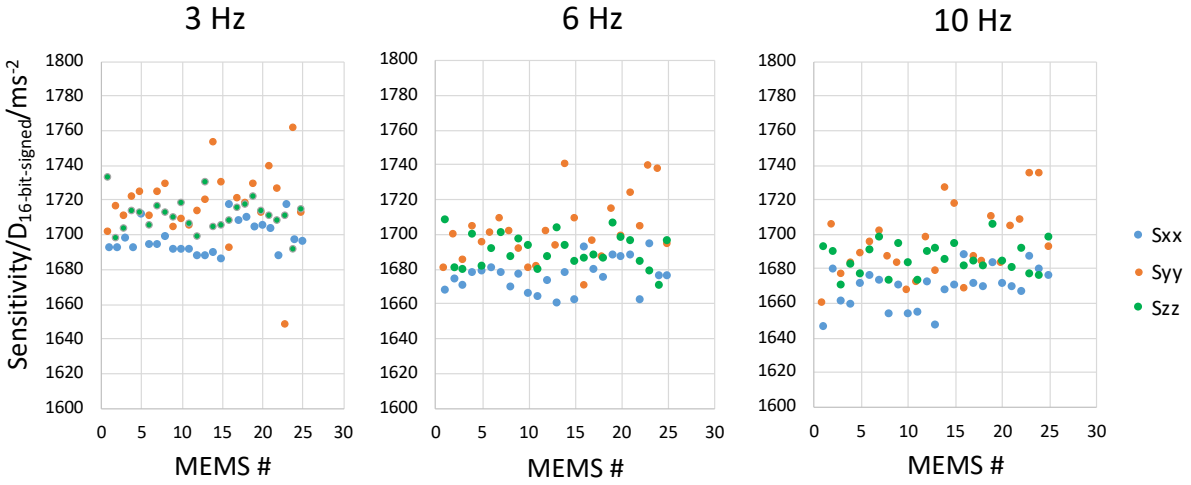

439

440 **Fig. 11**. Main sensitivities of the 25 MEMS at 3 Hz, 6 Hz and 10 Hz evaluated at UNIVAQ.

441

442 Transverse sensitivities of the 25 MEMS evaluated by the two laboratories are in the order of 1%-3% and
443 are depicted in Figs. 12 and 13 as boxplots. It is worth noting that transverse sensitivities evaluated by INRIM
444 in matrix form, also defined as cross-sensitivities, are part of the sensitivity of the sensor as they are used in
445 the exploitation equations [28], therefore values can be positive or negative.

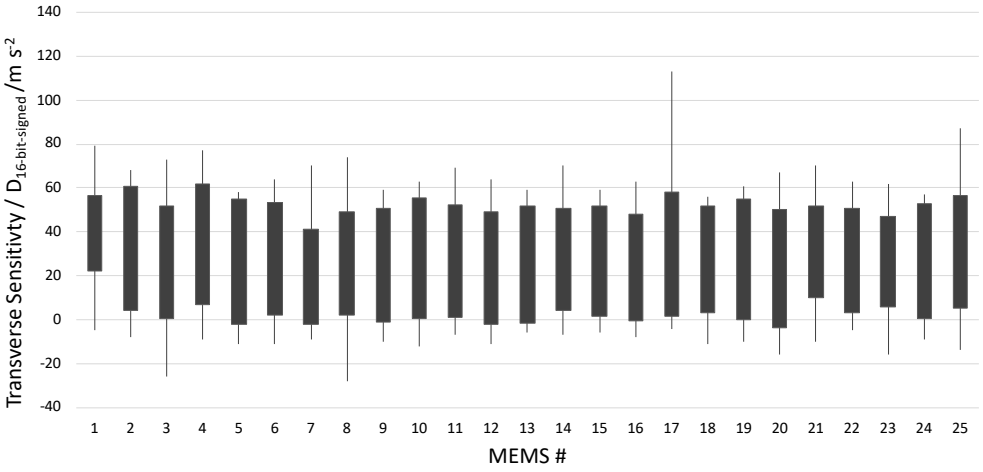

Fig. 12. Transverse sensitivity ranges of the 25 MEMS at 3 Hz, 6 Hz and 10 Hz evaluated at INRiM.

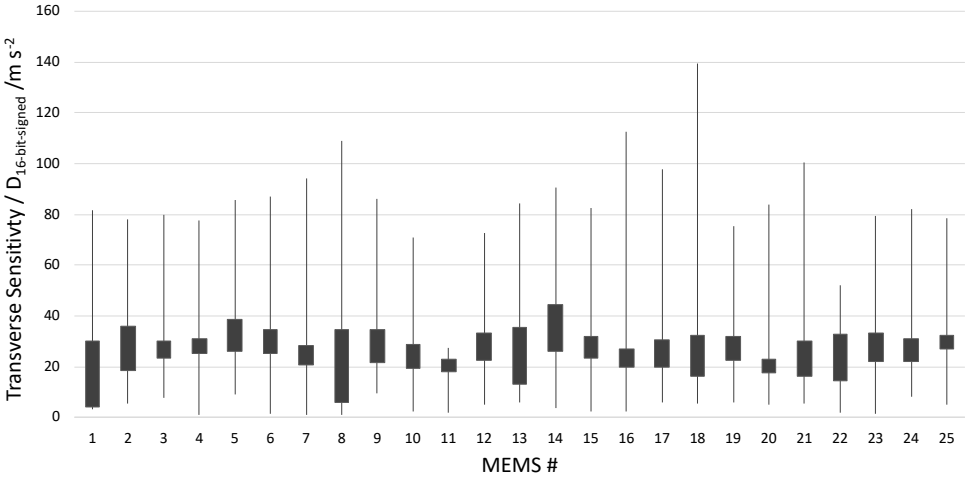

Fig. 13. Transverse sensitivity ranges of the 25 MEMS at 3 Hz, 6 Hz and 10 Hz evaluated at UNIVAQ.

An analysis based on the estimation of the normalized error (E_n), according to ISO/IEC 17043:2010 [51], is performed in order to assess the compatibility of the 25 MEMS sensitivity values, obtained from the two laboratories, for each axis and frequency under investigation. The data can be considered compatible when $E_n \leq 1$. Results, reported in Table 5, are compatible, although different mechanical excitation systems are used and different data analysis are adopted for the simultaneous determination of the sensitivities along the three axes. This result confirms the compatibility and the reproducibility of the two independent calibration systems for MEMS accelerometers within the metrological traceability chain.

464 **Table 5**

465 Normalized errors between INRIM and UNIVAQ

#	3 Hz			6 Hz			10 Hz		
	$E_n(S_{xx})$	$E_n(S_{yy})$	$E_n(S_{zz})$	$E_n(S_{xx})$	$E_n(S_{yy})$	$E_n(S_{zz})$	$E_n(S_{xx})$	$E_n(S_{yy})$	$E_n(S_{zz})$
1	0.40	0.34	0.71	0.22	0.24	0.76	0.08	0.12	0.28
2	0.34	0.53	0.55	0.33	0.62	0.56	0.50	0.67	0.90
3	0.09	0.63	0.27	0.48	0.35	0.53	0.03	0.40	0.21
4	0.02	0.29	0.52	0.65	0.69	0.92	0.31	0.45	0.29
5	0.53	0.63	0.55	0.18	0.77	0.52	0.11	0.47	0.37
6	0.28	0.09	0.53	0.44	0.45	0.88	0.53	0.52	0.72
7	0.41	0.42	0.79	0.62	0.44	0.89	0.44	0.35	0.72
8	0.70	0.39	0.65	0.59	0.59	0.63	0.05	0.29	0.35
9	0.33	0.29	0.28	0.80	0.45	0.30	0.32	0.50	0.55
10	0.05	0.35	0.42	0.52	0.24	0.34	0.13	0.21	0.19
11	0.09	0.40	0.59	0.04	0.45	0.44	0.22	0.49	0.51
12	0.09	0.44	0.33	0.24	0.90	0.33	0.23	0.68	0.52
13	0.21	0.51	0.62	0.22	0.54	0.54	0.19	0.40	0.42
14	0.03	0.41	0.11	0.11	0.57	0.81	0.10	0.70	0.34
15	0.01	0.35	0.40	0.21	0.46	0.32	0.46	0.66	0.78
16	0.28	0.12	0.28	0.41	0.26	0.46	0.43	0.34	0.50
17	0.28	0.53	0.52	0.28	0.51	0.91	0.40	0.51	0.66
18	0.52	0.41	0.51	0.52	0.21	0.16	0.34	0.34	0.20
19	0.34	0.46	0.22	0.16	0.51	0.52	0.46	0.50	0.59
20	0.43	0.50	0.41	0.29	0.83	0.52	0.25	0.48	0.25
21	0.48	0.63	0.26	0.36	0.49	1.00	0.14	0.47	0.47
22	0.11	0.46	0.41	0.53	0.69	0.80	0.19	0.53	0.68
23	0.49	0.42	0.19	0.53	1.00	0.21	0.40	0.71	0.00
24	0.09	0.82	0.18	0.38	0.64	0.63	0.53	0.83	0.35
25	0.49	0.25	0.52	0.31	0.42	0.83	0.80	0.47	0.54

466

467 **4. Discussion**

468 As stated in Section II, even a small sensor network implies a large number of sensitivity data to be managed
469 by end-users. By way of example, in this case, the sensitivity related to the sensor network, consisting of these
470 25 MEMS, entails a number of data from 225 (25 MEMS × 3 frequencies × 3 main sensitivity axes) up to 675
471 (if transverse sensitivities are also considered). Therefore, considering INRIM data as reference (Table 3), the

possibility of decreasing the number of sensitivities related to the sensor network is investigated. The idea is to perform different types of averages from the 225 main sensitivity data, in order to provide a lower number of sensor network sensitivities. Averages are performed in order that sensitivities are independent of MEMS, frequency or axis, or combination of these factors, up to the limit case of a single sensitivity value attributed to the whole sensor network independent from the three examined factors, the so-called ensemble sensitivity. In this way, the number of data to be managed is reduced, at the expense of an introduction of larger uncertainties and a loss of information about the influence of the investigated factors, but that can be accepted in several practical conditions and in this particular case of structural and infrastructures health monitoring and seismic safety networks at urban/building scale [52-54].

Mean sensitivities associated to the different combinations of these factors can be summarized in the following paragraphs. It is worth reminding that the sensitivity value declared by the manufacturer is 1671 $D_{16\text{-bit-signed}}$ /m s^{-2} and is reported in the following figures, as a continuous black line, for comparisons. For each case, uncertainties, in terms of expanded uncertainties *U* at a confidence level of 95%, are evaluated by performing the root sum squared of the maximum calibration uncertainty among the averaged data and the standard deviation of the averaged data. As a consequence, in this case, relative expanded uncertainties increase at increasing number of averaged data. However, in general, the data-set of sensitivity values, averaged as a function of MEMS, frequency or axes, show good compatibility, both in terms of mean values and associated expanded uncertainties, beyond to be consistent with the nominal sensitivity provided by the manufacturer.

However, preliminarily, an analysis of variance of the three factors (MEMS, axis and frequency) is performed in order to identify the main influencing effects on sensitivity. As a matter of fact, depending on the application, it can be useful to have a better resolution of vibration measurements as a function of frequency or direction of propagation. Results of analysis of variance, with sum of squares (SS), degree of freedom (DF) and Fisher's-Test *F* value, are reported in Table 6.

Table 6

Analysis of variance of sensitivity data

Factor	*SS*	*DF*	*F*	
MEMS	23771.01	24	0.8	
Freq.	119480.19	2	49.7	*
Axis	30480.99	2	12.7	*
MEMS × Freq.	17267.15	48	0.3	
MEMS × Axis	32680.35	48	0.6	
Freq. × Axis	1715.73	4	0.4	
MEMS × Freq. × Axis	30472.93	96	0.3	

Significant values at 95% confidence level are marked with * symbol. It is found that frequency and axis have a statistically significant effect on the sensitivity, whereas no influence due to the different MEMS sensors or due to interactions among the three factors is found. This is confirmed by the fact that, as average, standard

deviations of frequency and axis dependent sensitivities among all 25 MEMS are lower than MEMS dependent sensitivities, as shown as follows.

4.1 Ensemble sensor network sensitivity

The limit case of this approach is the evaluation of one single sensitivity to be attributed to the whole sensor network by calculating the mean value between sensitivity values of all MEMS. axes and frequencies. In this way, an «ensemble» sensitivity of 1659±72 $D_{16\text{-bit-signed}}/(m/s^2)$ is obtained and is reported in the following figures as grey lines (continuous line represents the mean value. dotted lines represent lower and upper limits). It should be noted that 72 $D_{16\text{-bit-signed}}=4.3\cdot10^{-2}$ m s^{-2}, in the MEMS configuration used in the investigation. It follows that, by using the ensemble sensitivity, the associated expanded uncertainty is around 4.5%.

4.2 MEMS dependent sensor network sensitivity

By averaging sensitivities of each single MEMS for all axes and frequencies. values reported in Fig. 14 are obtained. Given the similar sensitivity, due to the observed good compatibility among the 25 MEMS, mean values are close to the ensemble sensitivity of all 25 MEMS and it can be reasonably attributed to each single MEMS independently if specific frequency and axis information is not necessary. Associated relative expanded uncertainties are around 4.3%.

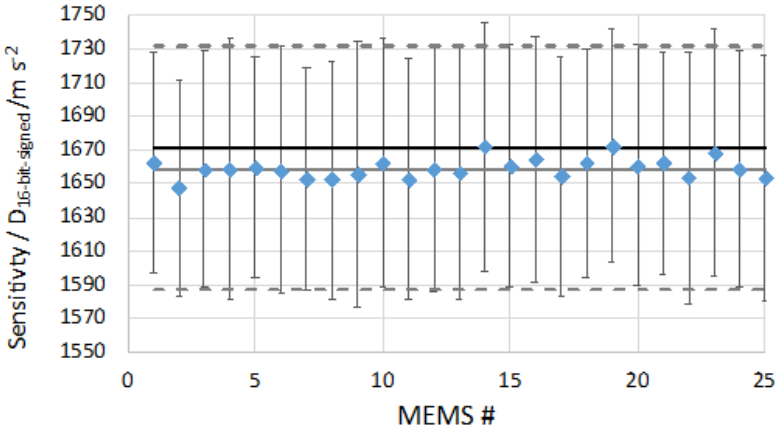

Fig. 14. Sensitivities of the 25 MEMS averaged for all frequencies and axes. Black line corresponds to the sensitivity declared by the manufacturer. Grey lines correspond to the ensemble sensitivity with lower and upper limits.

4.3 Frequency dependent sensor network sensitivity

By averaging the sensitivity values of the 25 MEMS as a function of frequency, the related sensitivity of the network is more trustworthy and accurate for frequency analysis of occurring vibration phenomena. In this case study the sensitivity is 1678±66 $D_{16\text{-bit-signed}}/(m/s^2)$ at 3 Hz. 1649±67 $D_{16\text{-bit-signed}}/(m/s^2)$ at 6 Hz and 1650±65 $D_{16\text{-bit-signed}}/(m/s^2)$ at 10 Hz, and relative expanded uncertainties are around 4%.

In the graph of Fig. 15, the values of frequency dependent sensitivities are shown, with respect to the nominal sensitivity and within the ensemble sensitivity lower and upper limits.

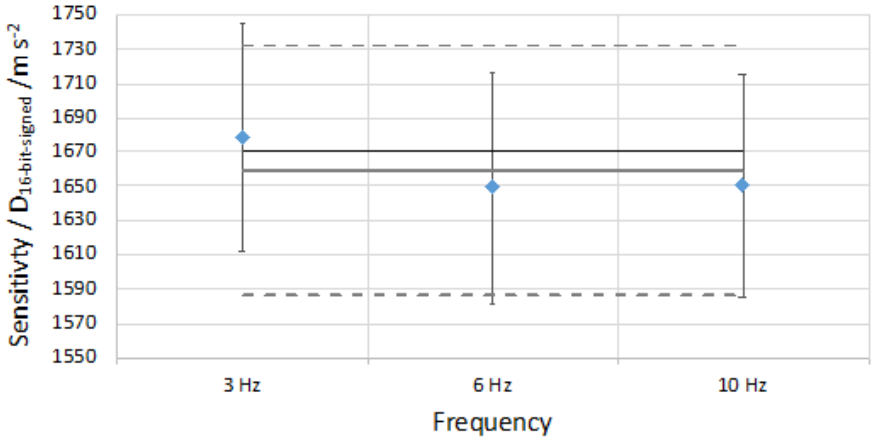

Fig. 15. Frequency dependent network sensitivity. Black line corresponds to the sensitivity declared by the manufacturer. Grey lines correspond to the ensemble sensitivity with lower and upper limits.

4.4 Axis dependent sensor network sensitivity

By averaging the sensitivity values of the 25 MEMS as a function of axis, the sensitivity of the network allows to define the direction of vibration propagation with a better resolution, with respect to frequency.

In this case study the sensitivity is 1657±71 $D_{16\text{-bit-signed}}/(m/s^2)$ for *x*-axis. 1653±72 $D_{16\text{-bit-signed}}/(m/s^2)$ for *y*-axis and 1668±50 $D_{16\text{-bit-signed}}/(m/s^2)$ for z-axis. Relative expanded uncertainties are around 3%-4%. In the graph of Fig. 16, the values of axis dependent sensitivities are shown, with respect to the nominal sensitivity and within the ensemble sensitivity lower and upper limits.

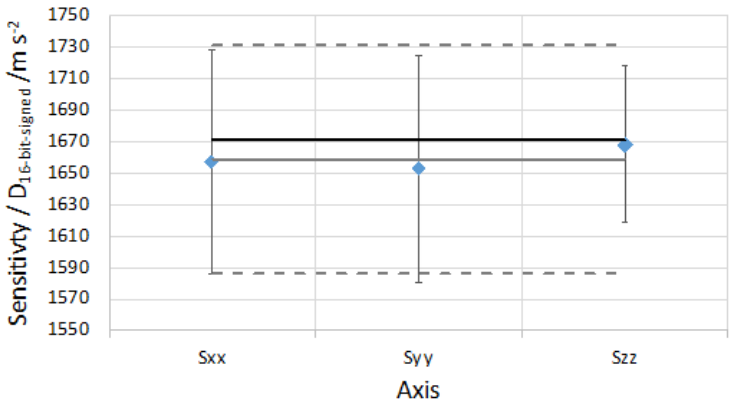

Fig. 16. Axis dependent network sensitivity. Black line corresponds to the sensitivity declared by the manufacturer. Grey lines correspond to the ensemble sensitivity with lower and upper limits.

4.5 Frequency and axis dependent sensor network sensitivity

An optimized compromise, in order to evaluate with a suitable trustworthiness both frequency response and direction of propagation of the vibration phenomena at the same time, by managing only 9 values of sensitivity data. can be achieved by defining the network sensitivity as a function of averaged frequency sensitivities and averaged axes sensitivities, as shown in the graph of Fig. 17. In this case study, the sensitivities in $D_{16\text{-bit-signed}}/(m/s^2)$ at 3 Hz, along *x*-, *y*- and *z*-axis, are, respectively, 1676±65, 1673±66 and 1686±42; at 6 Hz, are 1647±67, 1643±66 and 1657±46; and, at 10 Hz, are 1648±64, 1641±62 and 1663±42. Relative expanded uncertainties are between 2% and 4%.

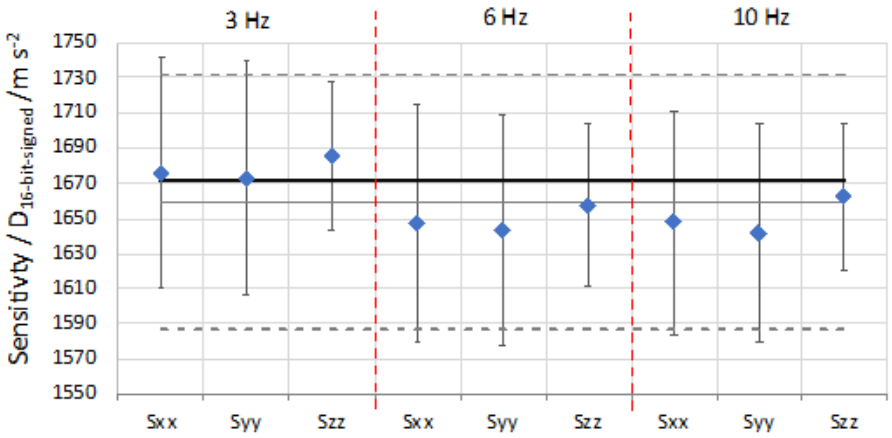

Fig. 17. Sensitivities of the 25 MEMS averaged for all frequencies and axes. Black line corresponds to the sensitivity declared by the manufacturer. Grey lines correspond to the ensemble sensitivity with lower and upper limits.

5. Conclusions

The increasingly widespread use of digital sensor networks. in many applications, including very sensitive ones (such as structural health monitoring), raises some important questions about the actual trustworthiness and accuracy of the data collected, in particular if neither standard calibration procedures nor traceable protocols are available for these sensors and for the interconnected network as a whole. In the field of metrology and measurement science, this fundamental topic begins to be investigated, with the aim of including these sensing infrastructures within the traceability chain, in analogy to traditional measuring instruments, therefore identifying their accuracy and trustworthiness, from adequate calibration systems and procedures, and supporting their compatibility and reproducibility, based on comparisons. In addition, the new developed procedures will have also to take into account both the low cost of the sensors and the huge quantity of MEMS produced, and they will have therefore to be adequately proportioned in such context.

In this work, the possibility of providing traceability, in terms of magnitude sensitivity, to digital MEMS accelerometers is investigated, on the basis of a rigorous metrological approach. The main purpose is to identify the problems inherent in calibration and to provide the relative possible solutions. Experimental data of the calibration of 25 MEMS accelerometers at 3 Hz, 6 Hz and 10 Hz, at nearly constant amplitude of 1 $m \cdot s^{-2}$, from two laboratories (NMI and University) are shown and compared. The resulting comparison gives useful information with reference to a possible procedure for calibration of MEMS tri-axis accelerometers. Different calibration methods are used, in terms of test benches, data processing techniques and reference standards, allowing to identify pros and cons of the specific approach. An analysis based on the estimation of the normalized error (E_n), according to ISO/IEC 17043:2010 shows compatible results at uncertainty levels between 2%-6%. This comparison allows to point out the aspects to be optimized into the procedure, concerning the management of the geometrical parameters of the devices used for calibration and the dynamic effects of test benches at low frequencies, to improve, in the future, calibration accuracy and further decrease the associated uncertainties.

Once the traceability of digital MEMS accelerometers is provided and the proper sensitivity (within the related uncertainty budget) is identified, a procedure to provide a suitable sensitivity to the sensor network as a whole is proposed, in order to decrease the number of sensitivity values to be managed by end-users. Different types of averages from the 225 main sensitivity data, in order that sensitivities are independent of MEMS, frequency or axis, or combination of these factors, up to the limit case of a single sensitivity value attributed to the whole sensor network, are proposed.

It is shown that, if a single value of sensitivity is used, independently on MEMS, axis and frequency of vibration, the associated uncertainty to this ensemble sensitivity is within 4.5%. Furthermore, the nominal value of sensitivity provided by the manufacturer is consistent with the obtained results, if this level of uncertainty is considered. Similar sensitivities appear among all the MEMS, if the same axes and frequencies are considered, while an increasing effect is acknowledged depending on the axis of vibration and on the vibration frequency, having the most relevant effects. An optimized compromise, in order to evaluate with a suitable trustworthiness both frequency response and direction of propagation of the vibration phenomena at the same time, by managing only 9 values of sensitivity data, instead of 225 single sensitivity values, can be achieved by defining the network sensitivity as a function of averaged frequency sensitivities and averaged axes sensitivities.

As a final remark, this work demonstrates the need of evaluating performances of MEMS as a single sensor or as a network, by a calibration procedure which takes into account carefully the main interfering aspects, in order to provide trustworthy and traceable data, within suitable coverage factors and uncertainties budgets, tailored to the actual needs of specific applications and employments.

Future work will be aimed at realizing a suitable calibration procedure for networks of digital MEMS accelerometers in terms of phase shift sensitivity, at evaluating the effects related to the different sampling rates

among MEMS sensors for dynamic applications, and finally at validating this MEMS accelerometers network in *in-field* applications.

Acknowledgements

The authors would like to thank Davide Lena, Camilla Mura and Andrea Labombarda. from the STMicro-electronics company, for the technical support, information and for the provision of the 25 digital 3-axis MEMS accelerometers.

References

[1] JCGM 200 2012 International Vocabulary of Metrology Basic and General Concepts and Associated Terms (VIM 3rd Edition) (France: Joint Committee for Guides in Metrology, Sévres).

[2] M. J. T. Milton and A. Possolo, Trustworthy data underpin reproducible research, Nature Physics 16(2) (2020) 117-119.

[3] A. Possolo and H. K. Iyer, Invited Article: Concepts and tools for the evaluation of measurement uncertainty, Review of Scientific Instruments 88(1) (2017) 011301.

[4] A. Possolo, Concepts, methods & tools enabling measurement quality, In: Proceedings of 13th International Workshop on Intelligent Statistical Quality Control 2019, IWISQC 2019, Hong Kong, Aug. 2019, pp. 195-214.

[5] IEEE Standard for Sensor Performance Parameter, IEEE Standard 2700-2017, Jan. 2018.

[6] Bureau International des Poids et Mesures - BIPM Strategy Plan (2018). [Online]
Available: https://www.bipm.org/utils/en/pdf/BIPM-strategic-plan-2018.pdf, Accessed on: Oct. 16, 2020

[7] BIPM - Consultative Committee for Acoustics, Ultrasound, and Vibration (CCAUV), Strategy plan 2019 to 2029, (2019). [Online].
Available: https://www.bipm.org/utils/en/pdf/CCAUV-strategy-document.pdf, Accessed on: Oct. 16, 2020

[8] BIPM - Consultative Committee on Electricity and Magnetism (CCEM), Strategic plan, (2014). [Online].
Available: https://www.bipm.org/utils/en/pdf/CCEM-strategy-document.pdf, Accessed on: Oct. 16, 2020

[9] BIPM - Consultative Committee for Length (CCL), Strategy 2018 2028, (2018). [Online].
Available: https://www.bipm.org/utils/en/pdf/CCL-strategy-document.pdf, Accessed on: Oct. 16, 2020

[10] BIPM - Consultative Committee for Mass and Related Quantities (CCM), Strategy 2017 to 2027, (2017). [Online].
Available: https://www.bipm.org/utils/en/pdf/CCM-strategy-document.pdf, Accessed on: Oct. 16, 2020

[11] ISO/IEC 17025:2018, General requirements for the competence of testing and calibration laboratories.

[12] J. Voas, Networks of 'Things', Natl. Inst. Stand. Technol. Spec. Publ. 800-183 (2016).

[13] PTB Communication, Metrology for the digitalization of the economy and society, (2017). [Online].

643 Available:
644 https://www.bipm.org/cc/PARTNERS/Allowed/2017_October/2017-Metrology-for-the-Digitalisation-of-
645 Economy-and-Society.pdf, Accessed on: Oct. 16, 2020
646 [14] MESAP "Smart Products and Manufacturing", [Online].
647 Available: https://www.mesap.it/mission/agenda-strategica/, Accessed on: Oct. 16, 2020
648 [15] D. Smorgon and V. Fernicola, A wireless reference node to provide self-calibration capability to wireless
649 sensors networks, In: Proc. Of ICST, Auckland, New Zealand, pp. 335-340, 2015.
650 [16] G. Crotti, A. Delle Femine, D. Gallo, D. Giordano, C. Landi, M. Luiso, and A. Scaldarella, A Method for
651 the Measurement of Digitizers' Absolute Phase Error, Journal of Physics: Conference Series, vol. 1065, no. 5,
652 pp. 052035, Aug. 2018, 10.1088/1742-6596/1065/5/052035
653 [17] G. Crotti, A. D. Femine, D. Gallo, D. Giordano, C. Landi and M. Luiso, Measurement of the Absolute
654 Phase Error of Digitizers, IEEE Transactions on Instrumentation and Measurement 68(6) (2019) 1724-1731.
655 DOI: 10.1109/TIM.2018.2888919.
656 [18] A. Prato, F. Mazzoleni and A. Schiavi, Metrological traceability for digital sensors in smart manufactur-
657 ing: calibration of MEMS accelerometers and microphones at INRiM, In: Proc of IEEE International Work-
658 shop on Metrology for Industry 4.0 and IoT, Napoli, Italy, 2019, pp. 371-375.
659 [19] M. Galetto, A. Schiavi, G. Genta, A. Prato and F. Mazzoleni, Uncertainty evaluation in calibration of low-
660 cost digital MEMS accelerometers for advanced manufacturing applications, CIRP Annals 68(1) (2019) 535-
661 538. DOI: 10.1016/j.cirp.2019.04.097.
662 [20] D. Smorgon, V. Fernicola, J. Sousa, L. Ribeiro, E. Tamburini and M. Catto, Assuring Measurement
663 Traceability to ATE Systems for MEMS Temperature Sensors Testing and Calibration, In: Proc. Of IEEE
664 International Workshop on Metrology for Industry 4.0 and IoT, Rome, Italy, 2020.
665 [21] EURAMET, "Publishable summary for 17IND12 Met4FoF metrology for the factory of the future," 2018.
666 [Online].
667 Available:https://www.ptb.de/empir2018/fileadmin/documents/em-
668 pir/Met4FoF/Docments/17IND12_Met4FoF_Publishable_Summary_M9.pdf, Accessed on: Oct. 16, 2020
669 [22] EURAMET, Publishable Summary for 17IND06 FutureGrid II Metrology for the next-generation digital
670 substation instrumentation, (2018). [Online].
671 Available: https://www.euramet.org/research-innovation/search-research-projects/details/project/metrology-
672 for-the-next-generation-digital-substation-instrumentation/?L=0&tx_eurametctcp_project%5Bac-
673 tion%5D=show&tx_eurametctcp_project%5Bcontroller%5D=Pro-
674 ject&cHash=3a961373b053be81eede260ad0b8b5fb, Accessed on: Oct. 16, 2020
675 [23] EURAMET, Publishable Summary for 17IND02 SmartCom Communication and validation of smart data
676 in IoT-networks, 2018. [Online].

677 Available: https://www.euramet.org/research-innovation/search-research-projects/details/project/communica-
678 tion-and-validation-of-smart-data-in-iot-networks/?L=0&tx_eurametctcp_project%5Bac-
679 tion%5D=show&tx_eurametctcp_project%5Bcontroller%5D=Pro-
680 ject&cHash=2341e12363c8623088e97fd7acf8872c, Accessed on: Oct. 16, 2020
681 [24] T. Bruns and S. Eichstädt, A smart sensor Concept for traceable dynamic measurements, Journal of Phys-
682 ics: Conference Series 1065(21) (2018) 212011. DOI: 10.1088/1742-6596/1065/21/212011.
683 [25] T. Dorst, B. Ludwig, S. Eichstädt, T. Schneider and A. Schütze, Metrology for the factory of the future:
684 towards a case study in condition monitoring, In: Proc I2MTC, Auckland, New Zealand, May 2019, pp. 1-5.
685 [26] B. Seeger, T. Bruns and S. Eichstädt, Methods for dynamic calibration and augmentation of digital accel-
686 eration MEMS sensors, In: Proc CIM2019, Paris, France, Sep. 2019, p. 22003.
687 [27] M. Mende and P. Begoff, Sensors with Digital Output - A Metrological Challenge, In: Proc CIM2019,
688 Paris, France, Sep. 2019, p. 22002.
689 [28] A. Prato, F. Mazzoleni, and A. Schiavi, Traceability of digital 3-axis MEMS accelerometer: simultaneous
690 determination of main and transverse sensitivities in the frequency domain, Metrologia 57(3) (2020) 035013.
691 DOI: 10.1088/1681-7575/ab79be
692 [29] A. Schiavi, F. Mazzoleni and A. Germak, Simultaneous 3-axis MEMS accelerometer primary calibration:
693 description of the test-rig and measurements, In: Proc XXI IMEKO World, Prague, Czech Republic, Sep.
694 2015.
695 [30] G. D'Emilia, A. Gaspari, E. Natale, F. Mazzoleni and A. Schiavi, Calibration of tri-axial MEMS accel-
696 erometers in the low-frequency range - Part 1: Comparison among methods, Journal of Sensors and Sensor
697 Systems 7(1) (2018) 245-257. DOI: 10.5194/jsss-7-245-2018.
698 [31] G. D'Emilia, A. Gaspari, E. Natale, F. Mazzoleni and A. Schiavi, Calibration of tri-axial MEMS accel-
699 erometers in the low-frequency range - Part 2: Uncertainty assessment, Journal of Sensors and Sensor System
700 7(1) (2018) 403-410. DOI: 10.5194/jsss-7-403-2018.
701 [32] G. D'Emilia, A. Gaspari and E. Natale, Amplitude–phase calibration of tri-axial accelerometers in the
702 low-frequency range by a LDV, Journal of Sensors and Sensor Systems 8 (2019) 223–231. DOI: 10.5194/jsss-
703 8-223-2019.
704 [33] G. D'Emilia, A. Gaspari, E. Natale, A simple method for amplitude/phase calibration of tri-axial accel-
705 erometers in the low frequency range, Journal of Physics Conference Series 1149(1) (2018) 012018.
706 [34] STMicroelectronics, "LSM6DSR," Mar. 2019. [Online].
707 Available: https://www.st.com/resource/en/datasheet/lsm6dsr.pdf, Accessed on: Oct. 16, 2020
708 [35] A. D'Alessandro, A. Costanzo, C. Ladina, F. Buongiorno, M. Cattaneo, S. Falcone, C. La Piana, S. Mar-
709 zorati, S. Scudero, G. Vitale, S. Stramondo and C. Doglioni, Urban seismic networks, structural health and
710 cultural heritage monitoring: the National Earthquakes Observatory (INGV, Italy) experience, Frontiers in
711 Built Environment 5(127) (2019). DOI: 10.3389/fbuil.2019.00127.

712 [36] S. Scudero, A. D'Alessandro, L. Greco and G. Vitale, MEMS technology in seismology: A short review,
713 In: Proc. 2018 IEEE International Conference on Environmental Engineering (EE), Milan, Italy, Mar. 2018,
714 pp. 1-5.
715 [37] M. C. Rodriguez-Sanchez, S. Borromeo and J. A. Hernández-Tamames, Wireless sensor networks for
716 conservation and monitoring cultural assets, IEEE Sensors Journal 11(6) (2010) 1382-1389. DOI:
717 10.1109/JSEN.2010.2093882.
718 [38] P. Ragam, and N. D. Sahebraoji, Application of MEMS-based accelerometer wireless sensor systems for
719 monitoring of blast-induced ground vibration and structural health: A review, IET Wireless Sensor Systems
720 9(3) (2019) 103-109. DOI: 10.1049/iet-wss.2018.5099.
721 [39] R. S. Concepcion, F. R. G. Cruz, F. A. A. Uy, J. M. E. Baltazar, J. N. Carpio and K. G. Tolentino, Triaxial
722 MEMS digital accelerometer and temperature sensor calibration techniques for structural health monitoring of
723 reinforced concrete bridge laboratory test platform, In: Proc HNICEM, Manila, Philippines, Dec. 2017, pp. 1-
724 6.
725 [40] D. Bhattacharyya, T. H. Kim and S. Pal, A comparative study of wireless sensor networks and their routing
726 protocols, Sensors 10(12) (2010) 10506-10523. DOI: 10.3390/s101210506.
727 [41] A. Dâmaso, N. Rosa and P. Maciel, Reliability of wireless sensor networks, Sensors 14(9) (2014) 15760-
728 15785. DOI: 10.3390/s140915760.
729 [42] M. A. Mahmood, W. K. Seah and I. Welch, Reliability in wireless sensor networks: A survey and chal-
730 lenges ahead, Computer Networks 79 (2015) 166-187. DOI: 10.1016/j.comnet.2014.12.016.
731 [43] C. Del-Valle-Soto, C. Mex-Perera, J. A. Nolazco-Flores, R. Velázquez and A. Rossa-Sierra, Wireless
732 Sensor Network Energy Model and Its Use in the Optimization of Routing Protocols, Energies 13(3) (2020)
733 728. DOI: 10.3390/en13030728
734 [44] STMicroelectronics, 32F769IDISCOVERY, (2016). [Online].
735 Available: https://www.st.com/resource/en/data_brief/32f769idiscovery.pdf, Accessed on: Oct. 16, 2020
736 [45] STMicroelectronics, private communication, (2020).
737 [46] ISO 16063-21, Methods for the calibration of vibration and shock transducers — Part 21: Vibration cali-
738 bration by comparison to a reference transducer, ISO (Geneva: International Organization for Standardization),
739 2003.
740 [47] JCGM 100, Evaluation of Measurement Data — Guide to the Expression of Uncertainty in Measurement
741 (GUM), Joint Committee for Guides in Metrology, Sèvres, France, 2008.
742 [48] A. Prato, A. Schiavi, F. Mazzoleni, A. Touré, G. Genta and M. Galetto, A reliable sampling method to
743 reduce large sets of measurements: a case study on the calibration of digital 3-axis MEMS accelerometers, In:
744 Proc. IEEE International Workshop on Metrology for Industry 4.0 and IoT, Rome, Italy, 2020.
745 [49] BIPM, KCDB, (2020). [Online].

Available:https://www.bipm.org/kcdb/cmc/search?domain=PHYSICS&areaId=1&key-words=&specificPart.branch=2&specificPart.service=7&specificPart.subService=15&specificPart.individu-alService=-1&_countries=1&countries=40&publicDateFrom=&publicDateTo=&unit=&min-Value=&maxValue=&minUncertainty=&maxUncertainty=, Accessed on: Oct. 16, 2020

[50] ISO 16063-31, Methods for the calibration of vibration and shock transducers — Part 31: Testing of transverse vibration sensitivity, ISO (Geneva: International Organization for Standardization), 2009.

[51] ISO/IEC 17043 Conformity assessment — General requirements for proficiency testing, ISO (Geneva: International Organization for Standardization), 2010.

[52] F. Lorenzoni, F. Casarin, M. Caldon, K. Islami and C. Modena, Uncertainty quantification in structural health monitoring: Applications on cultural heritage buildings, Mechanical Systems and Signal Processing 66 (2016) 268-281.

[53] R. Ferrari, F. Pioldi, E. Rizzi, C. Gentile, E. Chatzi, R. Klis, E. Serantoni and A. Wieser, Heterogeneous sensor fusion for reducing uncertainty in Structural Health Monitoring, 1st ECCOMAS thematic conference on uncertainty quantification in computational sciences and engineering (UNCECOMP 2015) 1 (2015) 511-528.

[54] L. J. Prendergast, M. P. Limongelli, N. Ademovic, A. Anžlin, K. Gavin and M. Zanini, Structural health monitoring for performance assessment of bridges under flooding and seismic actions, Structural Engineering International 28(3) (2018) 296-307.